33RD INTERNATIONAL COSMIC RAY CONFERENCE, RIO DE JANEIRO 2013
THE ASTROPARTICLE PHYSICS CONFERENCE

ICRC 2013

Newborn Pulsars as Sources of UHECRs and Their Neutrino Signatures

KE FANG[1], KUMIKO KOTERA[2], ANGELA V. OLINTO[1]

[1] *Department of Astronomy & Astrophysics, Kavli Institute for Cosmological Physics, The University of Chicago, Chicago, Illinois 60637, USA*
[2] *Institut dAstrophysique de Paris, UMR 7095 - CNRS, Universit e Pierre & Marie Curie, 98 bis boulevard Arago, 75014, Paris, France*

kefang@uchicago.edu

Abstract: Newborn pulsars can accelerate nuclei up to 10^{20} eV in their magnetosphere. The accelerated particles, which follow a unique E^{-1} energy spectrum at injection, further propagate through the surrounding supernova ejecta, and then reach the earth. The propagation softens the spectrum and generates a series of secondary particles as cosmic rays interact with the intervening backgrounds. With the proper injection composition, extragalactic pulsars can reproduce the energy spectrum and chemical composition (Xmax and RMS-Xmax) of ultrahigh energy cosmic rays observed by the Auger Observatory. In addition, the Galactic pulsar population can contribute significantly to cosmic rays between 10^{16} and 10^{18} eV, depending on the Galactic diffusion parameters. This contribution can bridge the gap between predictions of cosmic rays produced by supernova remnants and the observed spectrum and composition just below the ankle. The pulsar sources also produce high energy neutrinos, with flux and spectrum index dependent on the source properties. By average, pulsars that contribute to detectable neutrinos have a birthrate 1 per 1200 years.

Keywords: cosmic ray acceleration, neutron star, pulsar, supernova, ultrahigh energy cosmic ray, high energy cosmic ray, neutrino

1 Introduction

The origin of ultrahigh energy cosmic rays (UHECR) still remains a mystery [1]. The measurement of suppression at the highest energies [2] could be explained by the "GZK" cutoff [3] and/or the end of energies cosmic ray sources can accelerate to. Given the strength of Galactic magnetic fields and the lack of correlations with the Galactic plane, cosmic rays with energy above 2×10^{19} eV are most likely to be extragalactic [4]. The composition measurement by Pierre Auger Observatory [5] reports a puzzling trend from a light composition at a few EeV ($1\,\mathrm{EeV}=10^{18}$ eV) toward a heavy composition at around 60 EeV. This suggests a heavy nuclei dominated injection model, which is quite rare in the astrophysical literature of candidate sources. One may note however this composition trend is not confirmed by the Telescope Array [6].

Here we show that newborn pulsars as described in [8, 10, 12, 13] can explain the observed spectrum and composition of UHECRs(Section 2). High energy cosmic rays injected by pulsars in our own galaxy are discussed in Section 3. Finally in Section 4 we show the signatures and detectability of neutrinos emitted by galactic pulsars.

2 UHECR from Newborn Pulsars

In a pulsar born with magnetic dipole moment $\mu = 3\times10^{30}\,\mu_{30.5}\,\mathrm{erg/G}$, rotational speed $\Omega_i = 10^4\,\Omega_4\,\mathrm{s}^{-1}$, an iron nuclei with $Z = 26\,Z_{26}$ can be stripped off the star surface and accelerated to $E = 9\times10^{20}\,Z_{26}\,\eta_3\,\Omega_4^2\,\mu_{30.5}$ eV, assuming wind acceleration efficiency $\eta_3 \equiv \eta/0.3$ and star inertia $I = I_{45}\,10^{45}\,\mathrm{g\,cm^2}$ [10]. Assuming Goldreich-Julian charge density at the stellar surface [11], cosmic rays can be injected with a unique E^{-1} spectrum: $\mathrm{d}N_\mathrm{i}/\mathrm{d}E = 5\times10^{23}\,I_{45}(Z_{26}\,\mu_{30.5}\,E_{20})^{-1}\mathrm{eV}^{-1}$, ignoring the gravitational radiation. The timescale for particles to be accelerated to UHE reads $t_\mathrm{spin}\approx3\times10^7\left(3\times10^{20}\,\mathrm{eV}/E\right)Z_{26}\eta_1 I_{45}/\mu_{30.5}\,\mathrm{s}$.

The newly accelerated particles then travel through the dense supernova ejecta surrounding the neutron star. Assume the ejecta has a mass $M_\mathrm{ej,10} = M_\mathrm{ej}\,10\,M_\odot$, explosion energy $E_\mathrm{exp} = 10^{51}\,\mathrm{erg}$ and expands with velocity $\beta = \sqrt{2\,E_\mathrm{exp}/M_\mathrm{ej}\,c^2}$, the background optical depth for the nuclei is $\tau_{pp} = R_\mathrm{ej}/n_\mathrm{p}\sigma\kappa = 1.6\times10^5\,M_\mathrm{ej,10}\,\beta_{-1}^{-2}\,t_4^{-2}$, where $\beta_{-1} = \beta/0.1$, $t_4 = t/10^4\,\mathrm{s}$, assuming cross section $\sigma\sim10^{-25}\,\mathrm{cm}^2$ and elasticity $\kappa = 0.5$. In the simulation, we calculated the interaction between the nuclei and the hadron ejecta using a Monte-Carlo code [12]. The exact cross sections and interaction products are computed with EPOS [9].

The pulsar sources are known to be born with a distribution [14]. The initial spin period of the pulsar population is normally distributed with $\langle P\rangle = 300\,\mathrm{ms}$, $\sigma_P = 150\,\mathrm{ms}$, while the initial magnetic field follows a log-normal distribution with $\langle\log(B/\mathrm{G})\rangle = 12.65$ and $\sigma_{\log B} = 0.55$. On average the pulsar birth rate is $\Re\approx1/60\,\mathrm{yr}/\mathrm{Galaxy}$[7] and galaxy density $n_\mathrm{gal}\approx0.02\,\mathrm{Mpc}^{-3}$.

Summing up all the pulsars within the GZK horizon $c\,T_\mathrm{loss}\sim450\,\mathrm{Mpc}$ at $E_\mathrm{GZK} = 6\times10^{19}$ eV [1], the integrated spectrum and composition of UHECRs are shown in Figure 1. A mixed injection composition of 50% H, 30% CNO and 20% Fe was chosen to fit the Auger data [15]. The source emissivity is assumed to be constant over time. More results that provide fits to different data sets and source emissivity models are presented in [13].

The presence of secondary particles from interactions significantly softens the injected E^{-1} spectrum to $E^{-1.7}$. The source distribution further soften the intrinsic spectrum to around E^{-2}. In addition, the secondary products from a hadron interaction peak at energies roughly scaled to their mass number A, and therefor naturally present a transition from light to heavy in composition. The fit in

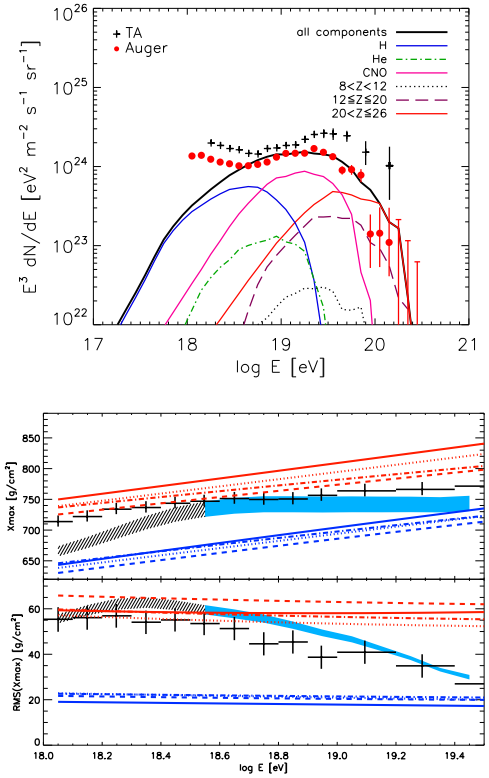

Figure 1: Propagated energy spectrum(up) and atmospheric depth $\langle X_{\rm max}\rangle$, its standard derivation rms($X_{\rm max}$)(bottom) of UHECRs produced by pulsar sources. Pulsars are assumed to be P, $\log\mu$ normally distributed and with wind acceleration efficiency $\eta = 0.3$. A mixed composition of of 50% P, 30% CNO and 20% Fe nuclei was injected to fit the Auger data [2]. Source emissivity is assumed to be uniform over time. The composition of different propagated nuclei are listed in the legends. Four interaction models, EPOSv1.99 [16], QGSJET01 [17], QGSJETII [18] and SIBYLL2.1 [19] were used to estimate the range of $\langle X_{\rm max}\rangle$ and rms($X_{\rm max}$).

Figure 1 results an overall normalization factor $f_s = 0.05$, which can be interpreted as the fraction of total flux of pulsar births required to account for the observed flux of UHECRs out of the total pulsar birth rate. $f_s < 1$ can be due to efficiency factors such as variations in the core-collapse geometry, poorer injection efficiency, or a lower hadronic density in the pulsar wind than the Goldreich-Julian density. The results do not sensitively dependent on injection composition. For example, the composition and spectrum after propagation remains nearly unchanged for an injection of 50% He, 30% CNO and 20% Fe[13].

Rotation powered neutron stars can only accelerate particles in the first $t_b \sim 12 Z_{26}\,\eta_3\, I_{45}\,\mu_{30.5}^{-1}$ yr in the pulsar's life time and thus are considered as transient sources. For one degree deflection over 100 Mpc, the time delay experienced by UHECRs in the intergalactic magnetic field is of order $\sim 10^4$ yrs, much longer than the time they get accelerated. No direct correlation between the arrival direction of events and an active source should be found. In large scale, distribution of arrival directions in the sky should trace the galaxy distribution with a possible bias [12].

3 Cosmic Rays from Galactic Pulsars

As an counterpart to extragalactic pulsars, the Galactic pulsars produce high energy cosmic rays. For the propagation of cosmic rays accelerated by Galactic pulsars, we model the turbulent Galactic magnetic field as a cylindrical halo of radius $R_{\rm Gal} = 15$ kpc, of height above (or below) the Galactic plane typically $H \sim 28$ kpc, of coherence length $lc \approx 10 - 100$ pc and strength $B = 3\,\mu$G [24]. At energies above the knee 10^{15} eV, nuclei spallation is negligible and the time nuclei stay in the Galaxy can be estimated with the Leaky box model $\tau_{\rm esc} = H^2/D$. The Galactic diffusion coefficient D is estimated empirically as in [25] $D(R, l_c) \sim r_{\rm L}\, c\left(r_{\rm L}/l_c + (r_{\rm L}/l_c)^{-2/3}\right)$. In the Kolmogorov regime when particles are totally diffusive (a charged particle's Larmor radius $r_{\rm L}$ much greater than l_c), $D(R) = 1.33\times 10^{28}\, H_{\rm kpc}\,(E/3\,{\rm GV})^{1/3}$ cm^{2}s^{-1}[26]. As R increases, $r_{\rm L}$ becomes greater than lc, then particles random walk with small deflections in the magnetic field. At extreme energies $\tau_{\rm esc} \geq H/c$, a third regime starts when the diffusion coefficient saturates to cH and particle travels quasi-rectilinearly.

The spectrum of cosmic rays produced by Galactic pulsars peak in between 10^{16} and 10^{18} eV (Figure 2 upper panel). Depending on the choice of Galactic diffusion parameters and dataset to fit with, Galactic pulsars may or may not dominate the Galactic cosmic ray flux below the ankle measured by Kascade [20]. This Galactic pulsar contribution can bridge the gap between predictions for cosmic ray acceleration in other Galactic sources, e.g. supernova remnants and the observed spectrum just below the ankle.

The bottom panel of Figure 2 contrasts the composition predictions of our models with the measurements by non-imaging Cherenkov detectors (Tunka, Yakutsk, CASA-BLANCA) and fluorescence detectors (HiRes/MIA, HiRes, KASKADE-GRANDE, Auger and TA) based on hadronic interaction model EPOSv1.99 (see [23] and references therein). The composition trends of our model reproduces some of the Galactic-Extragalactic transition features at the ankle as shown by the Auger and the KASKADE measurements. Below a few times 10^{17} eV, the composition is determined by other sources that dominate the flux. If the additional flux comes from acceleration in supernova remnants the composition is likely to be mostly heavy.

Assuming a homogeneous distribution of sources in the Galactic disc, the small-scale anisotropy signal can be estimated as $\sigma = 3/2^{3/2}\,\pi^{1/2}\,D(E)/Hc$ [26]. For the energy range pulsars contribute significantly (between $10^{16} - 10^{18}$ eV), the cosmic ray flux is mostly composed of CNO and Iron nuclei, that produce less anisotropy as they have smaller rigidity than protons at the same energy. In general our results are consistent with the anisotropy measurements [13].

4 Neutrinos from Pulsars in the Local Group

Neutrinos are produced when cosmic rays interact with background hadrons. The pions produced in the interaction decay to neutrinos when the ambience is diluted, and pion lifetime in the lab is shorter than pion-proton interaction time. That is, when the suppression factor $f_{\rm sup} = \frac{t_{\pi_{\rm p}}}{\gamma_\pi\,\tau_\pi}$ is larger than 1. If $f_{\rm sup} < 1$, pions participate in another hadron interaction rather than decay.

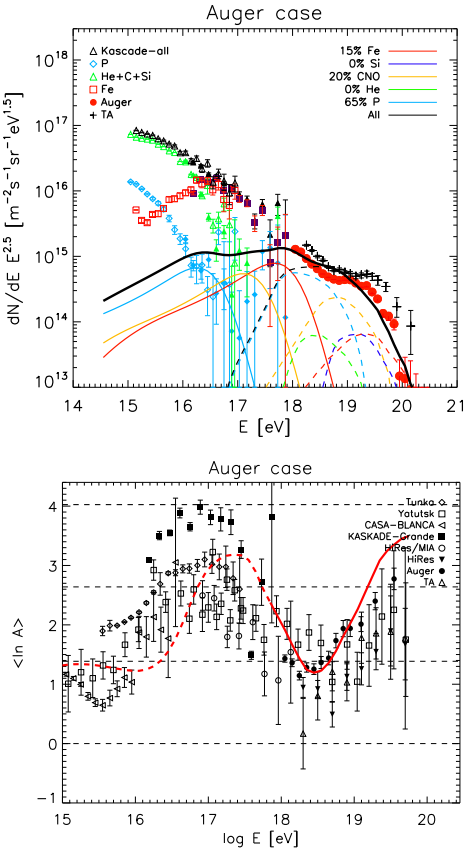

Figure 2: Cosmic ray flux measurements by KASCADE-Grande [20], Auger [22] and TA [21] compared with pulsar model predictions. The total spectrum in solid black sums up extragalactic (dash) and Galactic (solid) components. Pulsar and propagation parameters: all pulsars are assumed to inject cosmic rays with the same composition of of 65% P, 20% CNO and 15% Fe and with wind acceleration efficiency $\eta = 0.3$. Galactic halo height is $H = 2\,\mathrm{kpc}$ and coherence length of B-field is $lc = 20\,\mathrm{pc}$. Dashed lines indicate the energy range where pulsars contribute less than 80% to the total flux and other sources also contribute. Data from different detectors (see [23] and reference therein) are listed in the legends.

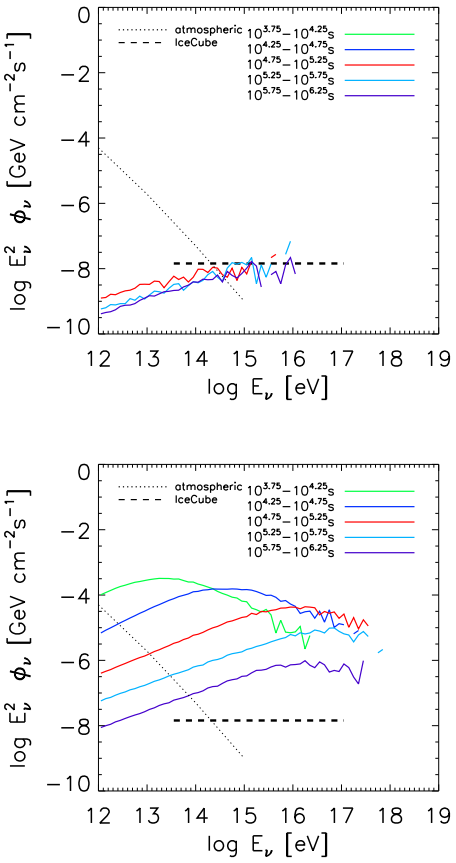

Figure 3: The ν_μ and $\bar{\nu}_\mu$ fluence from a newborn pulsar at 1 Mpc, at different time intervals as shown in the legend. The source is assumed to be a pulsar with surface magnetic field $B = 10^{12.65}\,\mathrm{G}$ and initial spin period $P = 10\,\mathrm{ms}$ in the upper panel, and a magnetar with $B = 10^{15}\,\mathrm{G}$, $P = 0.6\,\mathrm{ms}$ in the bottom panel. Acceleration efficiency is $\eta = 0.1$ for both cases. The flux is compared with atmospheric neutrino background (dotted) and IceCube upper limit (dashed) [27].

Assuming $t \gg \tau_{\rm EM}$, $f_{\rm sup} = 1$ happens at $t_{\rm had} = 2.3 \times 10^5\,\mathrm{s}\,\eta_{-1}^{1/4} M_{\rm ej,1}^{1/4} \mu_{33}^{-1/4} \beta_{-1}^{-3/4}$, assuming $\sigma_{\pi p} = 5 \times 10^{26}\,\mathrm{cm}^2$ and $\kappa_{\pi p} = 0.5$. Neutrinos peak at $E_{\nu,\rm peak} = E_\nu(t = t_{\rm had}) = 2.13 \times 10^{17}\,\mathrm{eV}\,\eta_{-1}^{3/4} M_{\rm ej,1}^{-1/4} \mu_{33}^{-3/4} \beta_{-1}^{3/4}$.

Figure 3 shows the neutrino emission level if a local pulsar at 1 Mpc bursts in the future. In the top panel, the source is assumed to be a pulsar with the average magnetic field strength $B = 10^{12.65}\,\mathrm{G}$ and initial spin period $P = 10\,\mathrm{ms}$. The neutrino emission is underdominant by atmospheric neutrinos below $5 \times 10^{14}\,\mathrm{eV}$. Over PeV the flux is comparable to the integral upper limit of IceCube $E^2\Phi_\nu = 3.6 \times 10^8\,\mathrm{GeV\,sr^1\,s^1\,cm^2}$ [27]. With the neutrino effective area for a 4π isotropic flux, 2 years lifetime, and the IC79 and IC86 string configurations [28], the predicted neutrino event number of this pulsar is ~ 1 at $3 - 10\,\mathrm{PeV}$.

In the bottom panel, the source is assumed to be a magnetar with $\mu = 10^{33}\,\mathrm{erg/G}$, corresponding to $B = 10^{15}\,\mathrm{G}$ and initial rotational speed $\Omega_{\rm i} = 10^4\,\mathrm{s}^{-1}$, corresponding to $P = 0.6\,\mathrm{ms}$. The neutrino level is well above IceCube limit in this case. The neutrino fluence peaks at 10 TeV at $t \approx 3\,\mathrm{hr}$, shifts to 1 PeV at $t \approx 8\,\mathrm{hr}$ and to 10 PeV at $t \approx 1\,\mathrm{day}$ with flux decreases afterwards. The typical spin down time of pulsars due to electro-magnetic radiation $\tau_{\rm EM}$ is much smaller than the time the source ambience gets optically thin $t = \left(n_{\rm p}\sigma\,\kappa\,c\right)^{-1} \sim 10\,\mathrm{year}$. The suppression factor $f_{\rm sup} \ll 1$ and thus unlike the injected E^{-1} spectrum, secondary pions and nuclei contribute significantly to neutrinos at low energies, and smooth the overall neutrino spectrum to about E^{-2}.

To produce neutrinos above 100 TeV pulsars need to have a spin period smaller than 10 ms. This corresponds to 5% of the pulsar population. By average every 1200 years a pulsar that contributes to measurable neutrino flux should be born in the local universe ($D \leq 1\,\mathrm{Mpc}$).

5 Conclusion

Newborn pulsars from nearby galaxies can be successful UHECR accelerators. The unique E^{-1} spectrum originating from the pulsar spin-down and heavy element injection from the neutron star allow a fit to both the energy spectrum and chemical composition measured by the detectors on Earth. Meanwhile, Galactic pulsars can produce high energy cosmic rays between 10^{16} and 10^{18} eV. This contribution adds to cosmic rays from other Galactic sources and balances the overall composition in the Galactic-Extragalactic transition region. By average every 1200 years, one pulsar with measurable neutrino signatures is born. The emitted neutrinos can have a E^{-1} spectrum if the typical spin down time of the pulsar $\tau_{\rm EM}$ is much larger than 10 years, or a $\sim E^{-2}$ spectrum if $\tau_{\rm EM} \ll 10$ years. If such high energy neutrino signals are detected in the future, it can serve as the smoking gun announcing the birth of high energy cosmic rays in newborn pulsars.

References

[1] K. Kotera, and A. V. Olinto, ARAA 49, 119153 (2011), 1101.4256
[2] R. U. Abbasi, et al., Physical Review Letters 100, 101101+ (2008). J. Abraham, et al., Physics Letters B 685, 239246 (2010), 1002.1975.
[3] J. E. Gunn, and J. P. Ostriker, Physical Review Letters 22, 728731 (1969). V. S. Berezinsky, and G. T. Zatsepin, Physics Letters B 28, 423424 (1969).
[4] G. Giacinti, M. Kachelriess, D. Semikoz, and G. Sigl, JCAP 1207, 031 (2012), 1112.5599.
[5] Pierre Auger collaboration, J. Abraham, et al., Measurement of the Depth of Maximum of Extensive Air Showers above 1018 eV, Phys. Rev. Lett. 104 (2010) 091101
[6] H. Tokuno, Y. Tameda, M. Takeda, K. Kadota, D. Ikeda, et al., Nucl.Instrum.Meth. A676, 5465 (2012), 1201.0002.
[7] D. R. Lorimer, Binary and millisecond pulsars, Living Rev. Relativ. 11 (2008) 8.
[8] P. Blasi, R. I. Epstein, and A. V. Olinto, ApJ Letters 533, L123L126 (2000) 9912240.
[9] Werner, K., Liu, F.-M., & Pierog, T. 2006, Phys. Rev. C, 74, 044902
[10] J. Arons, ApJ 589, 871892 (2003)
[11] P. Goldreich, and W. H. Julian, ApJ 157, 869+ (1969).
[12] K. Fang, K. Kotera, and A. V. Olinto, The Astrophysical Journal 750, 118 (2012), 1201.5197.
[13] K. Fang, K. Kotera, A. V. Olinto, 2013, JCAP, 3, 10
[14] C.-A. Faucher-Giguere, and V. M. Kaspi, ApJ 643, 332355 (2006)
[15] P. Abreu, et al. (2011), 1107.4809.
[16] T. Pierog and K. Werner, Muon Production in Extended Air Shower Simulations, Phys. Rev. Lett. 101 (2008) 171101.
[17] N. Kalmykov, S. Ostapchenko and A. Pavlov, Quark-gluon string model and EAS simulation problems at ultra-high energies, Nucl. Phys. Proc. Suppl. B 52 (1997) 17.
[18] S. Ostapchenko, Hadronic Interactions at Cosmic Ray Energies, Nucl. Phys. Proc. Suppl. 175-176 (2008) 73.
[19] E.-J. Ahn, R. Engel, T.K. Gaisser, P. Lipari and T. Stanev, Cosmic ray interaction event generator SIBYLL 2.1, Phys. Rev. D 80 (2009) 094003.
[20] KASCADE-Grande collaboration, W. Apel, et al., Kneelike structure in the spectrum of the heavy component of cosmic rays observed with KASCADE-Grande, Phys. Rev. Lett. 107 (2011) 171104
[21] Telescope Array collaboration, C.C. Jui, Cosmic Ray in the Northern Hemisphere: Results from the Telescope Array Experiment, J. Phys. Conf. Ser. 404 (2012) 012037
[22] Pierre Auger collaboration, P. Abreu, et al., The Pierre Auger Observatory II: Studies of Cosmic Ray Composition and Hadronic Interaction models, arXiv:1107.4804
[23] K.-H. Kampert and M. Unger, Measurements of the Cosmic Ray Composition with Air Shower Experiments, Astropart. Phys. 35 (2012) 660
[24] J.L. Han, New knowledge of the galactic magnetic fields, Nucl. Phys. Proc. Suppl. 175-176 (2008) 62 [arXiv:0901.0040] [INSPIRE].
[25] K. Kotera and M. Lemoine, Inhomogeneous extragalactic magnetic fields and the second knee in the cosmic ray spectrum, Phys. Rev. D 77 (2008) 023005
[26] P. Blasi and E. Amato, Diffusive propagation of cosmic rays from supernova remnants in the Galaxy. I: spectrum and chemical composition, JCAP 01 (2012) 010
[27] R. Abbasi et al. (IceCube Collaboration), Phys.Rev. D83, 092003 (2011).
[28] M.G.Aartsenetal. (IceCubeCollaboration),arXiv:1304.5356

This work was supported by the NSF grant PHY-1068696 at the University of Chicago, and the Kavli Institute for Cosmological Physics through grant NSF PHY-1125897 and an endowment from the Kavli Foundation.